Original Research Paper   **Open Access**

Enhanced Effluent Quality of Ceramic Membrane Ultrafiltration Combined with UV/TiO$_2$ Photocatalysis

Zhou Zhen*, Yao Jilun**†, Zhang Xing*, Ding Zhaoxia* and Zuo Meimei*

*Department of National Defense Architectural Planning and Environment Engineering, Logistical Engineering University, Chongqing, 401311, China

**Engineering and Technological Research Center of National Disaster Relief Equipment, Logistical Engineering University, Chongqing, 401311, China

†Corresponding author: Yao Jilun

ABSTRACT

To decrease ratio of the organic compounds in permeate water during micro-polluted surface water ultrafiltration process, UV/TiO$_2$ photocatalytic oxidation was employed as ceramic membrane ultrafiltration (CMU) pretreatment by elevation of the level of effluent quality. Initially, the catalytic activity between new and recycled TiO$_2$ was estimated by the degradation of COD$_{Mn}$. The data illustrate that the photocatalytic efficiency exhibits no crucial distinction of activity between unused and used titanium dioxide after decomposition. Secondarily, the decomposition of organic matter was explored through UV/TiO$_2$-CMU cycling test. The results illuminate that the concentration of COD$_{Mn}$ during the UV/TiO$_2$-CMU coupling technology is higher than the CMU technique. Conversely, the proportion of UV$_{254}$ in the yield of UV/TiO$_2$-CMU is lower than CMU. This phenomenon is ascribed to the low molecular weight organic matter, which is formed from macromolecule organic matter under incomplete photocatalytic dissociation. This micromolecule substance can easily penetrate membrane pores incurring the rising of COD$_{Mn}$ in UV/TiO$_2$-CMU hybrid system. Concurrently, this intermediate product is insensitive to ultraviolet light, diminishing the content of UV$_{254}$. Subsequently, parameters such as the reflux ratio, concentration of TiO$_2$, aeration rate, transmembrane pressure, and crossflow velocity that affected water quality in the hybrid process were investigated by single-factor experiments. Meanwhile, the main variables were optimized by orthogonal methodology using the removal of COD$_{Mn}$ as the response value. Optimal outcomes are attained at a reflux ratio of 85%, 0.5 g/L additional TiO$_2$, an aeration rate of 5 L/min, a transmembrane pressure of 0.05 MPa, and a crossflow velocity of 1.0 m/s.

INTRODUCTION

The membrane technology can be intrinsically elucidated as a physical sieve that winnows desired materials from admixture which are shoved by the pressure gradient or chemical potential field (Tian et al. 2011, Zhou et al. 2016a). Since it has been exploited to natural uranium enrichment in 1940s (Bhave 1911), ceramic membrane (CM) has been swiftly used in whole gamut of water treatment, by virtue of its unique mechanical structure, good chemical stability and long life span (Meng et al. 2011, Cao et al. 2013). For ceramic membrane ultrafiltration (CMU) process, one of the potential menace is the inferior effluent quality, when CMU treats micro polluted source water, like reservoir water or pond water that incorporates higher organic matter. There exists a range of nascent technologies that attempted to retard the pollution loading of CMU by pretreatment techniques such as magnetic flocculation (Pang et al. 2016a,b), electro-coagulation (Zhou et al. 2016b) or advanced oxidation (Bhatkhande et al. 2002).

Since the innovative work of Fujishima in 1972 (Fujishima et al. 1972), TiO$_2$ photocatalytic oxidation has engendered extensive attention for the ideal combination of chemical stability and active catalysis, high adsorption affinity and minimal outlay (Saqib et al. 2016, Jafari et al. 2016). When the surface of titanium dioxide is irradiated by UV light with energy tantamount to or greater than the bandgap energy, it induces the photo-generated electrons in the valance band (VB) to the conduction band (CB), leaving positive holes (h$^+$) and electrons (e$^-$) namely electron-hole pairs (Thiruvenkatachari et al. 2008, Mahlambi et al. 2015). The strong oxidizing of h$^+$ in the process of UV-TiO$_2$ photocatalytic oxidation could be applied to the mineralization of organic pollutants. The principal mechanism of titanium dioxide photocatalytic reaction is illustrated in Fig. 1.

However, the utility of powdered TiO$_2$ requires solid/liquid segregation, and the grave loss of catalytic titania curbs its widespread industrial applications. In the light of that weakness, we introduce the ceramic membrane ultrafil-

Fig. 1: Mechanism for TiO$_2$ photocatalytic oxidation.

Fig. 2: Flow chart of experimental set-up.

tration hybrid system to replace conventional physico-chemical methods such as filtration, centrifugation and co-agulation. This attempt may not only help in separating and recycling catalyst particles from solution efficiently, but also purifying permeate water and retarding membrane fouling effectually.

MATERIALS AND METHODS

Characteristics of lake water: The typical micro polluted source water was obtained from East Lake in Logistical Engineering University. During the entire gamut of experimental period, the original water had the temperature of 25.0-29.0°C, pH of 7.6-8.2, turbidity of 7.83-11.22 NTU, COD$_{Mn}$ of 6.06-7.57 mg.L^{-1} and UV$_{254}$ of 0.167-0.175 cm^{-1}.

Experimental equipment and reagents: A flow chart of the trial apparatus is sketched in Fig. 2. The photocatalytic reactor was made of stainless steel (800 mm in height, 200 mm in radius and 1 mm in thickness) with working volume of 22 L. A loop aeration pipe was fixed in the bottom of the photocatalytic cell with a mean pore size of 50 μm. Five 37 W UV tubes were selected as photo source with 254 nm dominant wavelength (ZW37D15Y(W)-Z793, Cn light optical-electrical technology Co. Ltd., Guangdong, China).

The ultrafiltration module (cross-flow filtering mode, Huicheng water treatment equipment Co. Ltd., Nanjing, China) consisted of two series-connected inner driving ceramic membranes (Al$_2$O$_3$) with the length of 500 mm. Pushed by a booster pump (40 m, 2.5 m^3/h, 450 W, Haobei mechanical-electrical equipment Co. Ltd., Shanghai, China), the original water flowed into, through 37 channels and then was winnowed by the thin ceramic membrane layer adhered to each raw water channel with nominal aperture of 50 nm. The sifted water was amassed in the filtrate ditches, then flowed out of the permeated collection grooves and eventually was stored in a 3 L backwash cylinder and permeate tank under ambient condition. To remove the membrane fouling, an air compressor was introduced.

The ordinary anatase TiO$_2$ powder (99% purity) was used

without further purification. The nominal size of this powder is 46 nm, but it cannot pass the 50 nm membrane pores because of the aggregation of TiO$_2$ particles in solution (Lei et al. 2009, Hua 2006, Weimin et al. 2001). The pH of the TiO$_2$ suspension was from 6.8 to 8.0.

Experimental methods: Before each test, the required operation parameters were adjusted using tap water. Initially, the immersible pump (15 m, 3.0 m^3/h, 550 W, GRUNDFOS) pumped raw water into the feed tank and mixed TiO$_2$ powder with the lake water. Secondarily, a feed pump pulled the admixture into the photocatalytic cell via feed pipe. Simultaneously, UV tubes offered the desired irradiation, and the micro-perforated aeration pipe supplied wanted gas flow powered by the air compressor. After that, the post-reaction mixture was injected into the ultrafiltration module through the booster pump. While the permeate water floated in the backwash cylinder and the permeate tank, the concentrating water was divided into two sections. One segment of the concentration was reflowed to photocatalytic cell to recycle the TiO$_2$ photocatalysts and enlarge the photo reaction time. The other portion of the compression was drained, according to the reflux ratio, controlled by the gate valve in the pipeline. In addition, the running parameters of transmembrane pressure and cross flow velocity were regulated through the valve in the outlet of the booster pump and the line of retention.

The water samples were acquired every 5 minutes. Subsequently, the turbidity was analyzed by HACH Model 2100AN and the UV absorbance in 254 nm was carried out in a rectangular quartz vessel using an ultraviolet spectrophotometer (Alpha-1506, spectrometer instrument Co. Ltd., Shanghai, China). Moreover, the content of COD$_{Mn}$ was measured with standard acid potassium permanganate titration method on the ground of Methods for Drinking Water-Aggregate Organic Parameters (GB/T 5750.7-2006, The State Environmental Protection Administration of China,
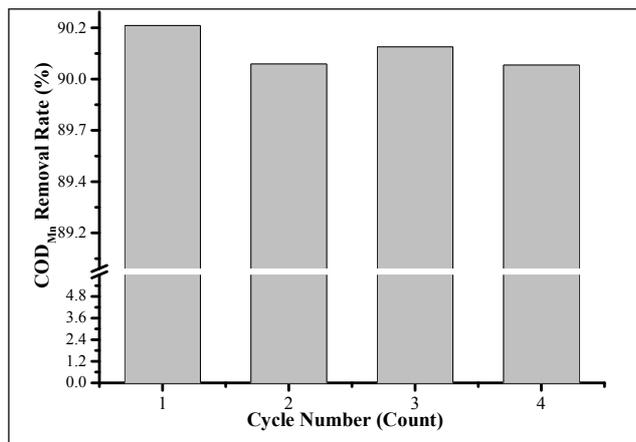
Fig. 3: Comparison between unused and used titanium dioxide in photocatalytic activity.

2006). To ensure the validity of these results, all data were reproduced twice before recording. Ultimately, to maintain the CMU neat, hydraulic backwashing and chemical circulation cleaning were performed with the help of the air compressor and the booster pump after each trial.

RESULTS AND DISCUSSION

TiO$_2$ photocatalytic activity test: To degrade organic compounds fuller in the process of photocatalytic oxidation, a massive amount of TiO$_2$ particles was needed. So, we wanted to minimise the operational investment by recycling some of the titania from the concentration using cross-flow filtering mode. But before taking action, it was incumbent upon us to ascertain whether the unused and used titanium dioxide had similar photodegradation capability, namely the stability of catalysts.

This test was carried out in a 1.5 L beaker in the presence of 0.5 g/L TiO$_2$ photocatalysts under 37 W UV light irradiation. The suspension was stirred magnetically during the photodegradation time (2 h). After each experiment, the content of COD$_{Mn}$ was analyzed and the white precipitate TiO$_2$ in the beaker was retrieved after clarification, filtration, rinsing, and finally dried in a drier at 60°C. The foregoing steps were reiterated for used TiO$_2$ and contrasted the impact with new TiO$_2$.

As is depicted in Fig. 3, all the titania showed high photocatalytic activities (COD$_{Mn}$ removal rate > 90% consistently) which manifested that the ability of photocatalysis was independent of cycle number in this experiment. Hence, recovering some of the titania from the concentrate was practicable.

UV/TiO$_2$-CMU cycling test: Although most sorts of organic compounds could be decomposed through TiO$_2$ photocata-

lytic process, long reaction time was needed. The reaction time, which specifically determined the volume of reactor required to reach a desired outcome, was a crucial factor in the devising of mobile water-purification devices. As the bulk of that mobile water-purification device was limited by the maneuverability, the level of photodegradation may not complete. For that reason, reaction time profiles of photodegradation of organic matter in UV/TiO$_2$-CMU cycling test are illustrated in Figs. 4 and 5. All the samples for measurements of COD$_{Mn}$ and UV$_{254}$ were maintained at 0.5 g/L of TiO$_2$ content, 5 L/min of aeration rate, 0.05 MPa of trans membrane pressure, and 1.5 m/s of cross flow velocity.

From 0 to 40 min, the content of COD$_{Mn}$ and UV$_{254}$ in the reactor was on a declining curve (Figs. 4 and 5) dropping nearly 25% and 50% respectively. Conversely, as can be seen from Fig. 4, the amount of COD$_{Mn}$ in filtered water was on a volcanic curve, which exhibited an upward trend before the climax of 5.39 mg/L COD$_{Mn}$ at 20 minutes and a downward tendency after the threshold value. Furthermore, comparison of CMU direct filtration with UV/TiO$_2$-CMU hybrid technique in the effluent quality, UV/TiO$_2$-CMU was inferior to CMU in terms of COD$_{Mn}$ removal while the former demonstrated preponderance in UV$_{254}$ elimination over the latter.

The culprit was the formation of micro-molecule intermediates during the incomplete photodegradation. According to Zhu et al. (2003), the degradation of organic compounds was performed by multiple elementary reaction gradually, and the reduction degree of organic matter was restricted to molecular weight, structure, and functional group. When humus was decomposed into organic compounds that contained functional groups such as phenyl, hydroxyl and double bond, higher percentage of hydroxyl radical was essential to curtail organic material. Furthermore, some kinds of functional groups had the priority to oxidize, causing the micro-molecule intermediates not be adequately eliminated in a finite time (Pramauro et al. 1993).

The second reason was pertinent to the adsorptive power of titanium oxide. Based on Langmuir-Hinshelwood's kinetic theory, the photocatalytic oxidation could be incised in adsorption and degradation and the previous step was vital to jump-start the reaction (Fu et al. 2005). The electrostatic attraction was the main driving force between anatase titanium dioxide and contaminants. It is generally accepted that TiO$_2$ is an amphoteric oxide. As depicted in Formula 1, massive groups of $\equiv$TiOH were formed by coordination in hydrolysis (Jiang 2007).

$$pH<pH_{zpc} \quad \equiv TiOH_2^+ \leftrightarrow \equiv TiOH + H^+$$
$$pH>pH_{zpc} \quad \equiv TiOH \leftrightarrow \equiv TiO^- + H^+ \quad ...(1)$$
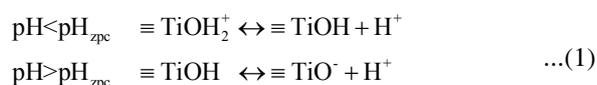
Fig. 4: Variation of COD_{Mn} in filtered water and reactor.
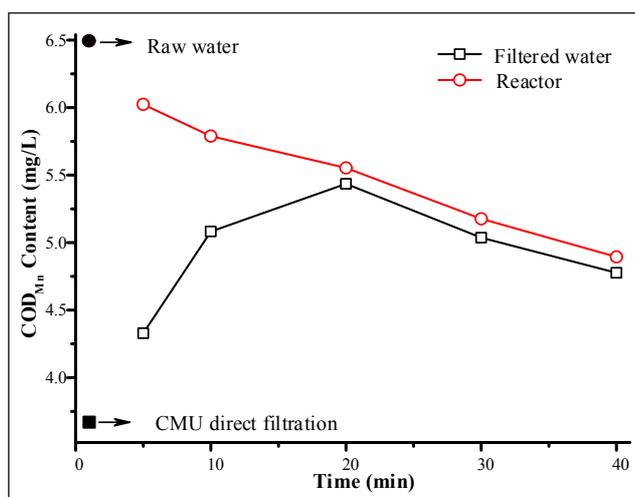

Fig. 5: Variation of UV_{254} in filtered water and reactor.

The hydrolyzed compound resemble to a dibasic acid. Since, the pH value of the solution (pH>7.5) outstripped the isoelectric point of TiO_2 (pH_{zpc}=6.3), the dominant product of the reaction was TiO^-. In theory, as shown in Formula 2, the process of photocatalytic oxidation is a pH-dropping procedure in the wake of OH^- depletion and gradual growth in H^+ (Cathy et al. 2011). Whereas, the dissertation of Yan (Yan 2009) reported the pH of the post-reaction solution to be steady about 7.0. Hence, surface of anatase TiO_2 displayed negatively charged in the slightly alkaline condition. The negatively charged particles there upon repulsed the micro-molecule intermediates which carried the same charge. The repulsive force was detrimental to the interaction between photocatalysis and organic intermediates. Then the pollutant was difficult to be degraded.

$$h^+ + OH^- \rightarrow \cdot OH$$
$$h^+ + H_2O \rightarrow \cdot OH + H^+ \qquad ...(2)$$

Thus, the aforementioned micro-molecule intermediates could punch through membrane pore inducing the jump of COD_{Mn} in permeate water.

As for UV_{254}, the consistently downward tendency was ascribed to the detection limit. Jiang and co-workers reported that the measurable valley molecular weight was 500 (Jiang & Liu 2002). So the component part (MW ≤ 500) of the organic midst in effluent cannot be measured. Fortunately, indicators, both COD_{Mn} and UV_{254}, in the reactor and effluent plummeted at the cycling time above 20 min. The above-mentioned phenomenon revealed that recurring operation was available to mobile water-purification device with limited space.

Single-factor experiments: *Effect of reflux ratio on effluent quality*: As was said before, we adopted the cycling strategy

to enhance oxidation efficacy. In the next section, we plumbed the critical factors (such as the reflux ratio, TiO_2 content, aeration rate, transmembrane pressure and cross flow velocity and so forth) to optimize the coupling techniques.

Initially, the effect of reflux ratio (from 85% to 100%) on effluent quality was probed in the presence of 0.5 g/L titania photocatalysts under 0.05 MP transmembrane pressure, 5 L/min aeration rate and 1.5 m/s cross flow velocity. The results are shown in Figs. 6 and 7.

It can be noted from Fig. 6 that the content of COD_{Mn} plummeted as the decrease in reflux ratio. When the proportion dropping to 85%, corresponding effluent COD_{Mn} was steady about 3.24 mg/L even if the percentage of COD_{Mn} elimination in filtrate was slightly deficient to the single CMU.

There are two causes responsible for that phenomenon. First, fewer yield of middle product. The lower level of reflux lead to more raw water entering into the reactor to keep a constant flow. Based on this, the shrinking retention period sunk the oxidation ability and then depressed the yield of middle product. Second cause is the higher emission of inter-medium. The relatively higher amount of middle product was drained, as the drainage of the concentrate.

Regarding the turbidity, the scale of it rapidly leaped from 10.37 NTU in lake water to 3300 NTU for additional TiO_2, while the effluent turbidity descended to 0.26 NTU behind single ultrafiltration. The inset in Fig. 7 signifies the corresponding turbidity variation curve as a function of reflux. The climbing polyline was owned to the loose structure of TiO_2 sediments. Tightness of that composition has positive correlation to reflux rate significantly (Zhang 2010). Large reflux encouraged the photodegradation of contaminants and dropping pH value (Formula 2), thus
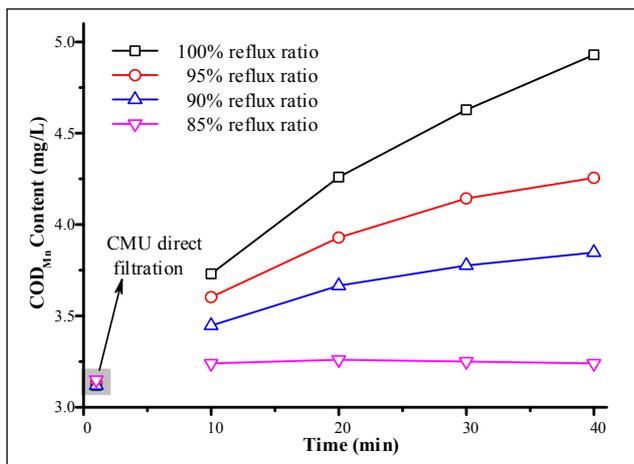
Fig. 6: Effect of reflux ratio on COD$_{Mn}$.

Fig. 7: Effect of reflux ratio on UV$_{254}$ and turbidity (inset).

facilitated the agglomeration of TiO$_2$ particles and growth of the cluster. The bigger-sized conglobated granulum was adversed to the interception of gel, and also aggravated the penetration of turbidity.

Effect of TiO$_2$ concentration on effluent quality: Secondarily, the resultant of TiO$_2$ concentration (from 0.3-1.1 g/L) on osmosis quality is recorded in Fig. 8 under the condition of 0.05 MPa transmembrane pressure, 1.5 m/s cross flow velocity, 85% reflux ratio, and 5 L/min aeration rate. The straight CMU filtration water had 3.23 mg/L COD$_{Mn}$ and 0.078 cm^{-1} UV$_{254}$.

It can be seen from Fig. 8, the trend of COD$_{Mn}$ removal is counter to UV$_{254}$ abatement. The reason for that state lay in the fact that increasing TiO$_2$ content promoted the adsorption quantity, reaction rate and micro-molecular organics formation in the primary stage. So the micro-molecule intermediates appeared in filtered water and surpassed the detection limits of optical methods, presenting an opposite tendency.

Whereas, it needs to be noted that the **edulcoration** of UV$_{254}$ drops off after 0.8 mg/L. It was probable that the efficiency of luminous energy utilization was poor for the robust scattering effect by excessive TiO$_2$ particles. Furthermore, an over-supply of TiO$_2$ generated a surging of agglomeration which weakened the reaction rate of photo oxidation. There upon, 0.5 g/L was chosen in ceramic membranes UF coupled with UV/TiO$_2$ process.

Effect of aeration rate on effluent quality: Fig. 9 presents the UF permeate quality (i.e., COD$_{Mn}$ and UV$_{254}$) following UV/TiO$_2$ at aeration rates (2-10 L/min) with a constant transmembrane pressure of 0.05 MPa, cross flow velocity of 1.5 m/s, and a TiO$_2$ concentration of 0.5 g/L with 85% reflux rate. The experimental lake water had 6.88 mg/L COD$_{Mn}$
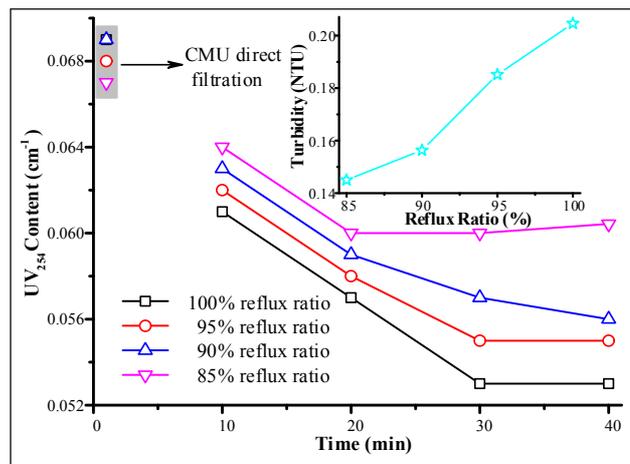
and 0.163 cm^{-1} UV$_{254}$ in these sections.

As with UV$_{254}$ absorbance, the removal percent rise linearly with increase in aeration before 8 L/min and then declines gently in the range of 8-10 L/min. For COD$_{Mn}$, its separation efficiency drops in the region of 2-8 L/min, and a slow enhancement after the critical point (8 L/min).

As we know, the influence of aeration in the reaction cell expresses two functions: (1) dispersing TiO$_2$ granule and (2) pumping oxygen. To some extent, the abnormal pattern of Fig. 9 is similar to Fig. 8 reflecting the aeration mechanism. As demonstrated in Formulas 3-5, the O$_2$ in the system not merely plays a role of electronic quenching agent, but also intensifies the formation of $\cdot$O$_2^-$ and H$_2$O$_2$, favoring photo oxidation progress. Also, inputting appropriately the air into the cell, promotes mass transfer, catalysts dispersion and adsorptive capacity for organic matter.

$$e^- + O_2 \rightarrow \cdot O_2^- \qquad \qquad ...(3)$$

$$\cdot O_2^- + H_2O \rightarrow HO_2 \cdot + OH^- \qquad \qquad ...(4)$$

$$2HO_2 \cdot \rightarrow H_2O_2 + O_2 \qquad \qquad ...(5)$$

But it needs to be noted that massive gas bubbles could squander valid ultraviolet radiation by light scattering which is adverse to reaction running. Consequently, the selected aeration rate of the reactor was 5 L/min.

Effect of transmembrane pressure on effluent quality: Transmembrane pressure is another important parameter for controlling the effluent quality in all filtration processes. In this experiment, the effect of transmembrane pressure in the coupling processes on the pollutant removal efficiency was investigated at a constant cross flow velocity of 1.5 m/s, TiO$_2$ concentration of 0.5 g/L, 85% reflux rate, and aeration rate of 5 L/min. While the initial characteristics of the pond were 6.92 mg/L COD$_{Mn}$ and 0.162 cm^{-1} UV$_{254}$.
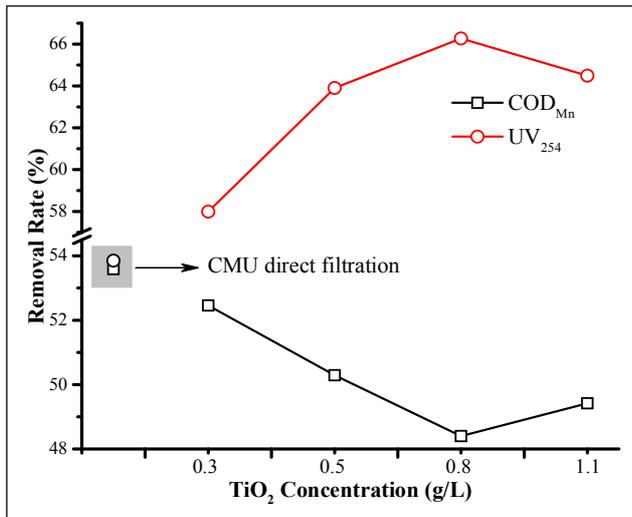
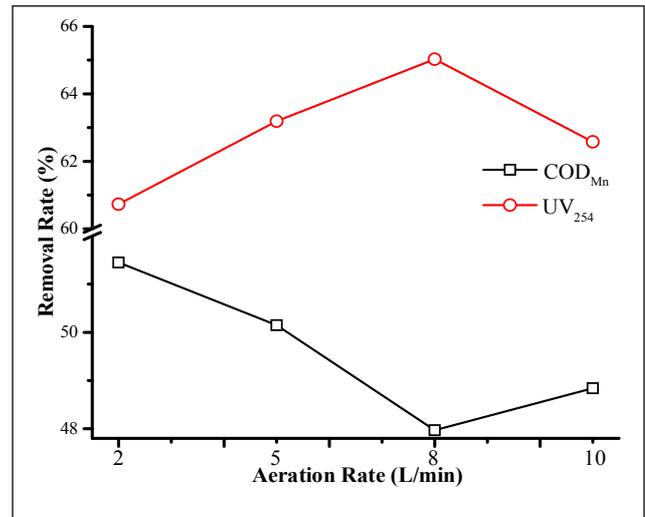Fig. 8: Effect of TiO$_2$ concentration on effluent quality.

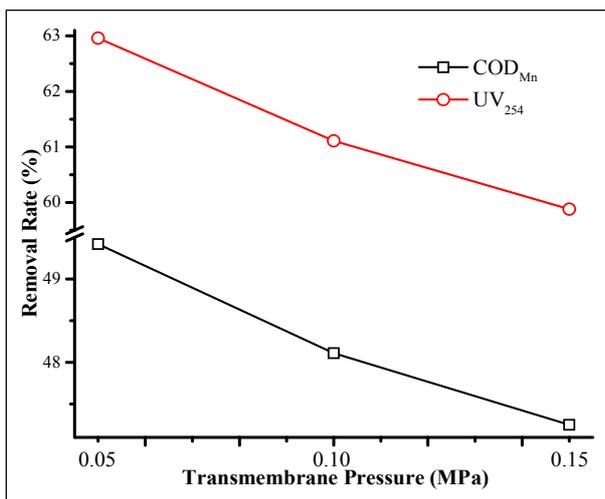Fig. 9: Effect of aeration rate on effluent quality.

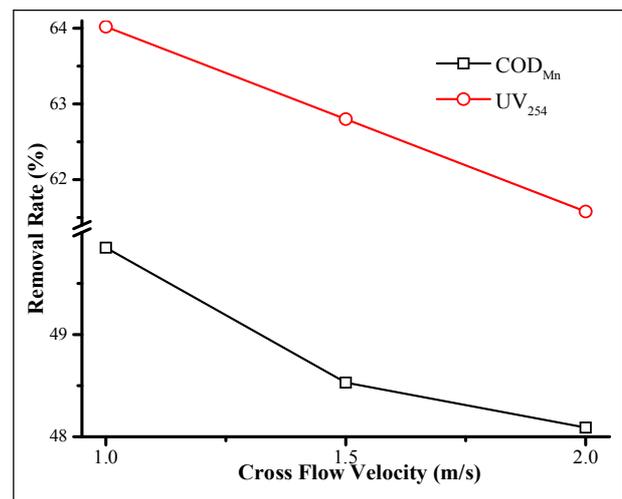Fig. 10: Effect of transmembrane pressure on effluent quality.

Fig. 11: Effect of cross flow velocity on effluent quality.

Variation of COD$_{Mn}$ and UV$_{254}$ removal in the hybrid process presented in Fig. 10, reveals that the organic substances elimination descend monotonously as transmembrane pressure increases. The reason is that the pressure affects the output of permeate water and input raw water. On one hand, higher input water restrained the retention period in the cell and the insufficient reaction time resulted in inadequate organic removal effectiveness. On the other hand, the higher amount of water needs to be filtered, the organic particle has more chance to pass through the membrane barrier, and aggravating interception loads of membrane. Hence, 0.05 MPa of transmembrane pressure was picked.

Effect of cross flow velocity on effluent quality: Cross flow velocity was explored at the range of 1.0 to 2.0 m/s in titania

content of 0.5 g/L, transmembrane pressure of 0.05 MPa, aeration rate of 5 L/min, and 85% reflux rate. In the primary stage, the raw water had 6.82 mg/L COD$_{Mn}$ and 0.164 cm^{-1} UV$_{254}$.

Fig. 11 sketches the change of COD$_{Mn}$ level and UV$_{254}$ as a function of cross flow velocity. It is clear that cross flow velocity has a marked effect on the removal of organic contaminants. The decreasing states in the graph were attributed to the whittling "secondary layer" effect (Arora & Davis 1994). Higher tangential fluid flow decreased the gel layer thickness in the vicinity of membrane surface, thus crippling the interception effect by ceramic membrane. To maintain effluent quality at a desirable ambit, 1.0 m/s was selected as the fine cross flow velocity.

Table 1: Factors and levels in orthogonal methodology.

F/actors Level	A/TiO$_2$ concentration (g/L)	B/aeration rate (L/min)	C/transmembrane pressure (MPa)	D/ cross flow velocity (m/s)
1	0.3	2	0.05	1.0
2	0.5	5	0.10	1.5
3	0.8	8	0.15	2.0

Table 2: Results of the orthogonal experiments.

Run	A/g/L	B/L/min	C/MPa	D/m/s	COD$_{Mn}$removal/%
1	0.3	2	0.05	1.0	51.81
2	0.5	5	0.10	1.5	51.78
3	0.8	8	0.15	2.0	51.56
4	0.5	2	0.10	2.0	52.04
5	0.5	5	0.15	1.0	52.84
6	0.5	8	0.05	1.5	52.71
7	0.8	2	0.15	1.5	49.01
8	0.8	5	0.05	2.0	52.38
9	0.8	8	0.10	1.0	51.65
COD$_{Mn}$ removal K$_1$	51.717	50.953	52.300	52.100	
K$_2$	52.530	52.333	51.820	51.167	
K$_3$	51.013	51.973	51.137	51.993	
R	1.517	1.380	1.163	0.933	

Table 3: ANOVA table for COD$_{Mn}$ removal rate.

Source	Sum square	Freedom degrees	F-value	Critical value	Significance
A	3.456	2	104.72	$F_{0.1}(2,2)=9.00$	***
B	3.316	2	100.48	$F_{0.05}(2,2)=19.00$	***
C	2.052	2	62.18	$F_{0.01}(2,2)=99.00$	**
D	1.566	2	47.45		**
Error	0.033	2			

Orthogonal methodology optimization: In this section, orthogonal methodology was taken to optimize operation variables based on COD$_{Mn}$ removal. Orthogonal test was conducted in four factors (TiO$_2$ concentration, aeration rate, transmembrane pressure and cross flow velocity) at three levels, as presented in Table 1.

The response figure of COD$_{Mn}$ was a stable average value during 1 h (sampling on every 10 min), as recorded in Table 2.

The results show that the range of those variables can be ranked as R$_A$ >R$_B$> R$_C$> R$_D$. According to the K$_{ij}$ (i=1,2,3; j=1,2,3,4) value, the refined operating conditions were A$_2$B$_2$C$_1$D$_1$, namely a reflux ratio of 85%, 0.5 g/L additional TiO$_2$, an aeration rate of 5 L/min, a transmembrane pressure of 0.05 MPa, and a cross flow velocity of 1.0 m/s.

Table 3 signifies the variance analysis of the experimental data. The source, C and D, having "**" in column six of Table 3 are significant at 95% confidence level. Meanwhile, A and B having "***" in the same column are highly significant to COD$_{Mn}$ elimination.

CONCLUSION

In this study, TiO$_2$ photocatalytic activity test, UV/TiO$_2$-CMU cycling test, single-factor experiment, and orthogonal methodology optimization were carried out to evaluate the combination technique on pollutants removal. The main findings are summarized below:

1. Used titanium dioxide has similar properties to the fresh one in photo oxidation.

2. Incompletely degraded intermediates may walk through membrane pores and increase COD$_{Mn}$ content in the filtrated water. The ostensibly decline of UV$_{254}$ in the filtration is due to insensitive intermediates in the condition of UV light.

3. The orthogonal optimization obtained the superior effluent quality at an aeration rate of 5 L/min, a transmembrane pressure of 0.05 MPa, a reflux ratio of 85%, a cross flow velocity of 1.0 m/s and 0.5 g/L additional TiO$_2$.

ACKNOWLEDGEMENTS

REFERENCES

Arora, N. and Davis, R.H. 1994. Yeast cake layers as secondary membranes in dead-end microfiltration of bovine serum albumin. Journal of Membrane Science, 92(3): 247-256.

Bhatkhande, D.S., Pangarkar, V.G. and Beenackers, A.A. 2002. Photocatalytic degradation for environmental applications-a review. Journal of Chemical Technology & Biotechnology, 77(1): 102-116.

Bhave, R.R. 1991. Inorganic Membranes Synthesis, Characteristics and Applications. New York: Van Nostrand Reinhold, 1-9.

Cao, Y.M., Xu, H.Y. and Wang, J.Q. 2013. Development status and prospect of inorganic ceramic membrane in China. Membrane Science and Technology, 33(2): 1-5.

Cathy, M.C., Nathan, S., Morgan, A. and Peter, K.J.R. 2011. Photocatalytic reactors for environmental remediation: a review. Journal of Chemical Technology and Biotechnology, 86(8): 1002-1017.

Fujishima, A. and Honda, K. 1972. Electrochemical photolysis of water at a semiconductor electrode. Nature, 238(7): 37-40.

Fu, J.F., Ji, M. and Jin, L.N. 2005. Factors affecting degradation of acid blue 7 by using photocatalysis-ultrafiltration separation reactor. Chemical Industry and Engineering Progress, 24(8): 916-924.

Hua, H.R. 2006. Study of photocatalysis-membrane filtration integrate process. Nanjing University of Science and Technology, 10-12.

Jafari, T., Moharreri, E., Amin, A.S., Miao, R., Song, W. and Suib, S.T. 2016. Photocatalytic water splitting-the untamed dream: a review of recent advances. Molecules, 21(7):1-29.

Jiang, S.J. and Liu, Z.Y. 2002. The meaning of UV_{254} as an organic matter monitoring parameter in water supply and wastewater treatment. Journal of Civil, Architectural and Environmental Engineering, 24(2): 61-65.

Jiang, Y.L. 2007. Modification of TiO_2/Ti catalyst and its photoelectric catalysis degradation of humic acid in water. Harbin Institute of Technology, 73-78.

Lei, L., Lu, N.N., Wu, M.H. and Qie, D.M. 2009. De-aggregation of nano-TiO_2 soft agglomeration in aqueous medium. Journal of Chemical Industry and Engineering (China), 60(12): 3159-3164.

Mahlambi, M.M., Ngila, C.J. and Mamba, B.B. 2015. Recent developments in environmental photocatalytic degradation of organic pollutants: the case of titanium dioxide nanoparticles-a review. Journal of Nanomaterials, 2: 1-29.

Meng, G.Y., Chen, C.S., Liu, W., Liu, X.Q. and Peng, D.K. 2011. Ceramic membrane technology: 30 years retrospect and prospect. Membrane Science and Technology, 31(3): 86-95.

Pang, Z.B., Yao, J.L., Liu, B. and Zhou, Z. 2016a. Experimental study on treatment of micro polluted raw water by combined process of magnetic flocculation and membrane filtration. Technology of Water Treatment, 42(4): 21-24.

Pang, Z.B., Yao, J.L., Liu, B. and Zhou, Z. 2016b. Optimization of magnetic flocculation and membrane filtration process with response surface method. Journal of Logistical Engineering University, 32(2): 62-66,71.

Pramauro, E., Vincenti, M., Augugliaro, V. and Palmisano, L. 1993. Photocatalytic degradation of Monuron in aqueous titanium dioxide dispersions. Environmental Science and Technology, 27(9): 1790-1795.

Saqib, N.U., Adnan, R. and Shah, I. 2016. A mini-review on rare earth metal-doped TiO_2 for photocatalytic remediation of wastewater. Environmental Science & Pollution Research, 23(16): 15941-15951.

Thiruvenkatachari, R., Vigneswaran, S. and Moon, I.S. 2008. A review on UV/TiO_2, photocatalytic oxidation process. Korean Journal of Chemical Engineering, 25(1): 64-72.

Tian, Y.L., Liu, G.Z., Yang, Y.Q., Gao, C.J., Yuan, D.D. and Li, R.Q. 2011. Research on inorganic membrane separation technology application in the field of water treatment. Environmental Protection Science, 37(6): 16-19.

Weimin, X. and Uwe, G.S. 2001. Separation of titanium dioxide from photocatalytically treated water by cross-flow microfiltration. Water Research, 35(5): 1256-1262.

Yan, X.J. 2009. Research on the performance and the mechanism of humic acid removal by the photocatalysis-membrane integrated process. Harbin Institute of Technology, 96-103.

Zhang, H. 2010. Photocatalysis and membrane separation hybrid system used in dyeing wastewatertreatment and reutilization. Zhejiang University of Technology, 53-58.

Zhou, Z., Yao, J.L., Pang, Z.B. and Liu, B. 2016a. Research progress on performance change of ceramic membrane for water treatment. Chemistry & Bioengineering, 33(2): 1-4.

Zhou, Z., Yao, J.L., Pang, Z.B. and Liu, B. 2016b. Mitigated fouling of ceramic microfiltration membrane by electrocoagulation pretreatment. Chinese Journal of Environmental Engineering, 10 (5): 2279-2283.

Zhu, X.L., Xie, Y.B. and Li, P. 2003. Research progress in the mechanism of nano-photocatalytic degradation of organics in water. Chemistry Online, 1: 10.